AIDIC *Conference Series*, Vol. 9, 2009
Editor Sauro Pierucci
DOI: 10.3303/ACOS0909020

ISBN 978-88-95608-10-5 ISSN 2036-5969

INTEGRATED MULTI-SCALE MODELS FOR MICROREACTOR SIMULATION AND DESIGN

Bostjan Hari, Florent Goujon and Constantinos Theodoropoulos*
School of Chemical Engineering and Analytical Science, University of Manchester, Manchester M60 1QD, U.K.

In this work we construct multi-scale models of continuous microreactors with Platinum (Pt) catalytic walls as an alternative to the conventional packed-bed configuration. The bulk (gaseous) phase is treated macroscopically using a reaction-diffusion model, while the catalytic activity is modelled at the micro/mesoscopic level using kinetic Monte Carlo (kMC) simulations including effects such as adsorption, desorption, surface reactions and surface diffusion. A number of kMC lattices depending on the discretisation of the computational domain are used to effectively represent the reactive surfaces. Time- and length-scales are coupled and results are compared to pure mean-field (MF) computations to validate the multi-scale approach.

1. INTRODUCTION

Microreactor systems are receiving increasing attention nowadays due to their enhanced operation characteristics such as increased mass and heat transfer capabilities, uniform flow, inherent safety and potential for high throughput through the construction of array configurations. They also ensure a smaller plant size, lower cost of production and more flexible response to market demand (Ehrfeld et al., 2000). Catalytic microreactors can be designed following the "traditional" packed-bed configuration which is well-tested but suffers from pore-plugging which is enhanced at diminishing dimensions. Alternatively, a catalytic wall concept, following the design of deposition reactors used for the production of microelectronics and functional materials such as self-cleaning glasses can be adopted. Models for such reactors need to be able to describe both the bulk (gas-phase) and the catalytic (surface) phenomena taking place at different lenth- and time-scales. Traditional mean field (MF) models cannot always accurately capture such complex dynamics possibly resulting in lack of understanding of the interactions underpinning the system and consequently in sub-optimal designs. The aim of this work is to develop a multi-scale model for catalytic microreactors that uses a macroscopic MF approach for the bulk phase coupled with the microscopic kMC on a lattice method to describe the surface dynamics. While a small numbers of such models have been developed (e.g. Raimondeau and Vlachos, 2002, Majumder and Broadbelt, 2006) distributed microreactors have not been investigated. The well-known system of *CO* oxidation is used as a test case and comparisons with pure MF predictions are used to validate the multi-scale model.

2. THE MULTI-SCALE MODEL

The multi-scale microreactor model consists of a MF model for the bulk phase coupled with a number of kMC lattice models that describe the catalytic surface. Alternatively the surface chemical reactions are modelled using a conventional MF model which is also coupled with the bulk phase macroscopic model for comparison purposes. A ternary gaseous system consisting of CO, O_2 and CO_2 is considered. A convection-diffusion model is used to describe the gas phase. The corresponding equation for mole fraction i, is given by

* Corresponding author: e-mail: k.theodoropoulos@manchester.ac.uk, FAX: +441612367439

Please cite this article as: Hari B., Goujon F. and Theodoropoulos C., (2009), Integrated multi-scale models for simulation and design, AIDIC Conference Series, 09, 167-176 DOI: 10.3303/ACOS0909020

$$c\cdot\left[\frac{\partial X_i}{\partial t}+v_x\frac{\partial X_i}{\partial x}+v_y\frac{\partial X_i}{\partial y}\right]=c\cdot D_{i,mix}\cdot\left[\frac{\partial^2 X_i}{\partial x^2}+\frac{\partial^2 X_i}{\partial y^2}\right]+r_i \qquad i=1,2 \tag{1}$$

where $c[mol/m^3]$ is the total concentration, $D_{i,mix}\left[m^2/s\right]$ is the diffusivity of the mixture, $X_i[-]$ is mole fraction of the gas species i and $v_x[m/s], v_y[m/s]$ are velocities in x and y directions. The diffusion coefficient for the gaseous mixture is calculated with equation (2) by using a mixture-average approximation and the relevant binary diffusion coefficients $D_{ij}\left[c\,m^2/s\right]$ are approximated with the Fuller equation (3) (Poling et al., 2001) as

$$D_{i,mix}=\frac{1-Y_j}{\sum_{j=1}^{n}\frac{X_j}{D_{ij}}} \tag{2}$$

$$D_{ij}=\frac{0.00143\cdot T^{1.75}}{p\cdot M_{ij}^{0.5}\cdot\left[\left(\sum_v\right)_i^{1/3}+\left(\sum_v\right)_j^{1/3}\right]^2} \tag{3}$$

$Y_j[-]$ is the mass fraction of species j, $T[K]$ is the temperature, $p[bar]$ is the pressure of the binary mixture and $\left(\sum_v\right)_i[-]$ is the atomic diffusion volume for each component (Poling et al., 2001). $M_{ij}=2\cdot\left[1/M_i+1/M_j\right]^{-1}\left[kg/kmol\right]$ is the binary molecular weight of homogeneous species i and j.
The total mass balance is given by equation (4).

$$\sum_{i=1}^{3}X_i=1 \tag{4}$$

The system of equations (1) to (4) is solved using the finite difference method (FDM). *CO* and O_2 diffuse onto the microreactor's Pt catalytic wall, where they adsorb to form surface species, which react on the surface and desorb to produce CO_2.

2.1 Surface Mean Field Model

The *CO* oxidation mechanism (Raimondeau and Vlachos, 2002) is shown in Table 1.

Table 1: *CO* oxidation surface mechanism

Surface Reactions	*CO* Model
Unimolecular adsorption	$CO+*\xrightarrow{k_{a1}}CO^*$
Unimolecular desorption	$CO*\xrightarrow{k_{d1}}CO+*$
Dissociative adsorption	$O_2+2*\xrightarrow{k_{a2}}2O^*$
Associative desorption	$2O^*\xrightarrow{k_{d2}}O_2+2*$
Bimolecular surface reaction	$CO^*+O^*\xrightarrow{k_{sr}}CO_2+2*$

A mean field (MF) model for catalytic *CO* oxidation is described by equations (5) and (6). The coverage of empty sites θ_* is obtained from the conservation of all surface species (7)

$$\frac{\partial\theta_{CO*}}{\partial t}=k_{a1}\cdot\frac{N_A}{c_T}\cdot c\cdot X_{CO}\cdot\theta_*-k_{d1}\cdot\theta_{CO*}-k_{sr}\cdot\theta_{CO*}\cdot\theta_{O*}$$
$$-k_{diff}\cdot\theta_{CO*}\cdot\theta_*+k_{diff}\cdot\theta_{CO*}\cdot\theta_* \tag{5}$$

$$\frac{\partial\theta_{O*}}{\partial t}=2\cdot k_{a2}\cdot\frac{N_A}{c_T}\cdot c\cdot X_{O_2}\cdot\theta_*^2-2\cdot k_{d2}\cdot\theta_{O*}^2-k_{sr}\cdot\theta_{CO*}\cdot\theta_{O*}, \tag{6}$$

$$\theta_{CO^*} + \theta_{O^*} + \theta_* = 1 \tag{7}$$

Here θ_{CO^*}, θ_{O^*} are the coverages of CO* and O* species respectively, $C_T\left[sites/m^2\right]$ is the density of surface sites and $N_A\left[molecules/mol\right]$ the Avogadro number. The corresponding rate constants for the above *CO* mechanism are (Raimondeau and Vlachos, 2002)

$$k_{a1} = s_{0,a1} \cdot \sqrt{\frac{1000 \cdot R \cdot T}{2\pi \cdot M_{CO}}} \tag{8}$$

$$k_{d1} = A_{0,d1} \cdot exp\left(\frac{-E_{a,d1}}{R \cdot T}\right) \tag{9}$$

$$k_{a2} = s_{0,a2} \cdot \sqrt{\frac{1000 \cdot R \cdot T}{2\pi \cdot M_{O_2}}} \tag{10}$$

$$k_{d2} = A_{0,d2} \cdot exp\left(\frac{-E_{a,d2}}{R \cdot T}\right) \tag{11}$$

$$k_{sr} = A_{0,sr} \cdot exp\left(\frac{-E_{a,sr}}{R \cdot T}\right) \tag{12}$$

where $R\left[J/(mol \cdot K)\right]$ is the ideal gas constant, $M_{CO}\left[kg/kmol\right]$ and $M_{O_2}\left[kg/kmol\right]$ are the molecular weights of *CO* and O_2, $s_{0,i}[-]$ is the sticking coefficient, $A_{0,i}\left[l/s\right]$ is the pre-exponential factor and $E_{a,i}\left[J/mol\right]$ is the activation energy. A two-dimensional microreactor, represented with a single microchannel is schematically shown in Figure 1. Here only the south boundary wall is assumed to be catalytic.

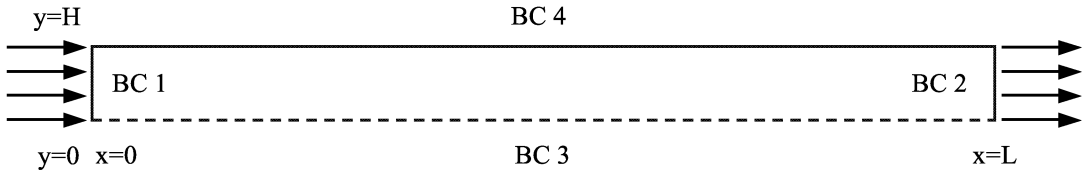

Figure 1: A mean-field microreactor model and the corresponding boundary conditions.

For the MF model, the corresponding MF boundary conditions (BCs) are shown in Table 2. BC 4 depicts the non-zero diffusive flux $\left[mol/\left(m^2 \cdot s\right)\right]$ at the catalytic surface given by

$$\frac{\partial X_{CO}}{\partial y} = \frac{k_{a1} \cdot X_{CO} \cdot \theta_* - k_{d1} \cdot \frac{c_T}{c \cdot N_A} \cdot \theta_{CO^*}}{D_{CO,mix}} \tag{13}$$

$$\frac{\partial X_{O_2}}{\partial y} = \frac{2 \cdot k_{a2} \cdot c \cdot X_{O_2} \cdot \theta_*^2 - 2 \cdot k_{d2} \cdot \frac{c_T}{c \cdot N_A} \cdot \theta_{O^*}^2}{D_{O_2,mix}} \tag{14}$$

$$\frac{\partial X_{CO_2}}{\partial y} = \frac{-k_{sr} \cdot \frac{c_T}{c \cdot N_A} \cdot \theta_{CO^*} \cdot \theta_{O^*}}{D_{CO_2,mix}} \tag{15}$$

Table 2: Initial and boundary conditions of a mean field microreactor model.

Boundary	Initial and Boundary Conditions
BC 1	$v_{x,in} \neq 0$, $v_{y,in} = 0$, $X_{CO,in} \neq 0$, $X_{O_2,in} \neq 0$
BC 2	$\frac{\partial v_{x,out}}{\partial x} = 0$, $v_{y,out} = 0$, $\frac{\partial X_{CO,out}}{\partial x} = \frac{\partial X_{O_2,out}}{\partial x} = 0$
BC 3	$v_{x,n} = 0$, $v_{y,n} = 0$, $\frac{\partial X_{CO,n}}{\partial y} = \frac{\partial X_{O_2,n}}{\partial y} = 0$
BC 4	$v_{x,s} = 0$, $v_{y,s} = 0$, $\frac{\partial X_{CO,s}}{\partial y} \neq 0$, $\frac{\partial X_{O_2,s}}{\partial y} \neq 0$

2.2 Surface Lattice Kinetic Monte Carlo Model

We have used a series of kinetic Monte Carlo (kMC) models describing surface reactions on two-dimensional nano-scale lattices to represent the microreactor catalytic surface. Modelling of each lattice is based on statistical probabilities. Expressions for the rate constants are (Reese et al., 2001; Raimondeau and Vlachos, 2002)

$$k_{a1} = \frac{s_{0,a1} \cdot N_A \cdot p_{CO}}{c_T} \cdot \sqrt{\frac{1000}{2 \cdot \pi \cdot M_{CO} \cdot R \cdot T}} \tag{16}$$

$$k_{d,1} = A_{0,d1} \cdot \exp\left(\frac{-E_{a,d1}}{R \cdot T}\right) \tag{17}$$

$$k_{a2} = \frac{s_{0,a2} \cdot N_A \cdot p_{O_2}}{c_T} \cdot \sqrt{\frac{1000}{2 \cdot \pi \cdot M_{O_2} \cdot R \cdot T}} \tag{18}$$

$$k_{d,2} = A_{0,d2} \cdot \exp\left(\frac{-E_{a,d2}}{R \cdot T}\right) \tag{19}$$

$$k_{sr} = A_{0,sr} \cdot \exp\left(\frac{-E_{a,sr}}{R \cdot T}\right) \tag{20}$$

The probabilities $P_{CO^*}[-]$, $P_{O^*}[-]$ and $P_*[-]$ for one site involving a single surface species CO^*, O^* or a vacant site, *, are (Reese et al., 2001):

$$P_{CO^*} = \frac{\Omega_{CO^*}}{\Omega_T} \tag{21}$$

$$P_{O^*} = \frac{\Omega_{O^*}}{\Omega_T} \tag{22}$$

$$P_* = \frac{\Omega_*}{\Omega_T} \tag{23}$$

where $\Omega_{CO^*}[-]$, $\Omega_{O^*}[-]$ and $\Omega_*[-]$ are the number of surface (catalyst) sites occupied by CO^*, O^* and *, respectively. $\Omega_T[-]$ is the total number of catalyst (lattice) sites. $P_{O^*/CO^*}[-]$ and $P_{CO^*/O^*}[-]$ represent the two-site class conditional probability of choosing a site O^*, once a site CO^* has been picked and vice versa

$$P_{O^*/CO^*} = \frac{\sum_{i=1}^{4} i \cdot \left(\Omega_{CO^*-O^*-i}\right)}{4 \cdot \Omega_{CO^*}} \tag{24}$$

$$P_{CO^*/O^*} = \frac{\sum_{i=1}^{4} i \cdot \left(\Omega_{O^*-CO^*-i}\right)}{4 \cdot \Omega_{O^*}} \tag{25}$$

$\Omega_{CO^*-O^*-i}[-]$ denotes the size of class CO^*-O^*-i, which means the number of sites of CO^* having i adjacent sites of O^* and similarly for $\Omega_{O^*-CO^*-i}[-]$. Transition probabilities $\hat{\Gamma}_i[-]$ for each reaction are summarized in equations (26) to (30). The total transition probability $\hat{\Gamma}_{tot}[-]$ is the sum of all individual probabilities.

$$\hat{\Gamma}_{a1} = k_{a1} \cdot p_{tot} \cdot X_{CO} \cdot P_* \tag{26}$$

$$\hat{\Gamma}_{d1} = k_{d1} \cdot P_{CO^*} \tag{27}$$

$$\hat{\Gamma}_{a2} = k_{a2} \cdot p_{tot} \cdot X_{O_2} \cdot P_* \cdot P_{*/*} \tag{28}$$

$$\hat{\Gamma}_{d1} = k_{d1} \cdot P_{CO^*} \cdot P_{CO^*/CO^*} \tag{29}$$

$$\hat{\Gamma}_{sr} = k_{sr}\left(P_{CO^*} \cdot P_{O^*/CO^*} + P_{O^*} \cdot P_{CO^*/O^*}\right) \tag{30}$$

$$\hat{\Gamma}_{tot} = \sum_{i=1}^{n_r} \hat{\Gamma}_i \tag{31}$$

Here $n_r[-]$ is the total number of events on a lattice. The reaction to occur in the current time-step is chosen through a random number, R_1 , according to the transition probabilities in conjunction with equation (32), while a second random number, R_2 , helps to compute the time-step $\Delta t[s]$ as shown in equation (33) for the next reaction event in the kMC lattice

$$\sum_{k=1}^{j-1} \hat{\Gamma}_k \langle R_1 \cdot \hat{\Gamma}_{tot} \langle \sum_{k=1}^{j} \hat{\Gamma}_k \tag{32}$$

$$\Delta t = \frac{1}{\Omega_T \cdot \hat{\Gamma}_{tot}} \cdot \log\left(\frac{1}{R_2}\right) \tag{33}$$

The multi-scale catalytic microreactor FD – kMC model using an array of kMC lattices, to represent the Pt catalytic south boundary, is depicted in Figure 2. Catalytic kMC lattices are coupled to the microreactor gas-phase FD model through partial pressures and adsorption/desorption reaction rates. kMC simulations yield surface coverages and the corresponding adsorbed and desorbed gas particles, for each kMC reporting horizon. The net number of gas particles coming into (adsorbing) and leaving (desorbing) the catalytic surface is used to

compute the corresponding macroscopic rates needed by BC4, which essentially provides the length-scale coupling in the model:

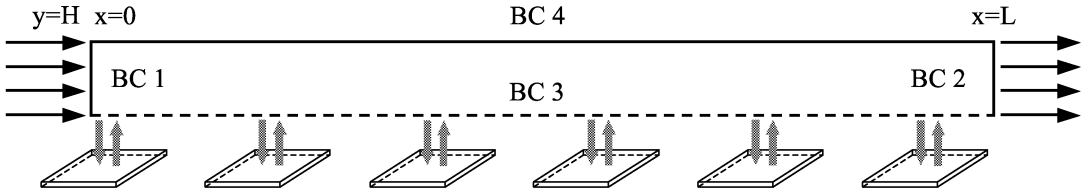

Figure 2 A FD-kMC microreactor model with an array of "catalytic" kMC lattices.

$$\frac{\partial X_i}{\partial y} = -\frac{rate_i}{c \cdot D_{i,mix}} \qquad i = 1,2,3 \tag{34}$$

All kMC lattices run for a reporting horizon using Message Passing Interface (MPI) parallelisation. The MF gas-phase model is then executed for the same time horizon and this iteration is repeated until the final chosen time. The appropriate boundary conditions used in the multi-scale model are shown in Table 3. BC3 provides the coupling between the gas-phase and the catalytic south surface/boundary.

Table 3: Initial and boundary conditions of a multi-scale microreactor model.

Boundary	Initial and Boundary Conditions
BC 1	$v_{x,in} \neq 0$, $v_{y,in} = 0$, $X_{CO,in} \neq 0$, $X_{O_2,in} \neq 0$
BC 2	$\frac{\partial v_{x,out}}{\partial x} = 0$, $v_{y,out} = 0$, $\frac{\partial X_{CO,out}}{\partial x} = \frac{\partial X_{O_2,out}}{\partial x} = 0$
BC 3	$v_{x,n} = 0$, $v_{y,n} = 0$, $\frac{\partial X_{CO}}{\partial y} = -\frac{rate_{CO}}{c \cdot D_{CO,mix}}$, $\frac{\partial X_{O2}}{\partial y} = -\frac{rate_{O2}}{c \cdot D_{O2,mix}}$, $\frac{\partial X_{CO2}}{\partial y} = -\frac{rate_{CO2}}{c \cdot D_{CO2,mix}}$
BC 4	$v_{x,s} = 0$, $v_{y,s} = 0$, $\frac{\partial X_{CO,s}}{\partial y} \neq 0$, $\frac{\partial X_{O_2,s}}{\partial y} \neq 0$

3. RESULTS AND DISCUSSION

MF and multi-scale simulations for *CO* oxidation in a catalytic microreactor were performed for 0.1 bar and 1.01295 bar at 700 K, with inlet velocity v=0 m/s (purely diffusion-driven flow). The two-dimensional microchannel was *9 mm long with a height of 1 mm*. Initial surface coverage in both models was set to zero. The initial gas-phase composition was X_{CO}=*0.2*, X_{O2}=*0.8*, while the inlet BC was set to X_{CO}=*0.1*, X_{O2}=*0.9*. 32 kMC lattices, of size *100x100 μm* each, were used to represent the catalytic surface in the multi-scale model with equal gaps between adjacent kMC lattices. Lattice kMC simulations are averaged over three copies in order to reduce the stochastic noise of the solution. A time step of *0.001 s* was used and results are shown at *0.01 s* and *0.2 s*, respectively. Surface coverages in Figure 3a and Figure 4a were found to exhibit similar trends for both models at different operating conditions. However, quantitative differences of approximately 0.1 can be observed in Figure 3a and 4a between the MF and the multi-scale models. At *0.1 bar* and *0.2 s*, the system has nearly reached steady state and the catalytic surface is almost fully covered with *O**, which is not the case for *1.01295 bar*, where steady state has not been reached and both *CO** and *O** are present on the surface. The gaseous mole fractions on the catalytic surface predicted by both, MF and the FD–kMC models are very close without significant differences. Overall, the multi-scale microreactor FD – kMC model can provide accurate predictions of the system complex behaviour and has the potential to provide a better understanding of the surface reaction mechanism. Furthermore, it can significantly contribute to the improvement of general microreactor design.

(a)

(b)

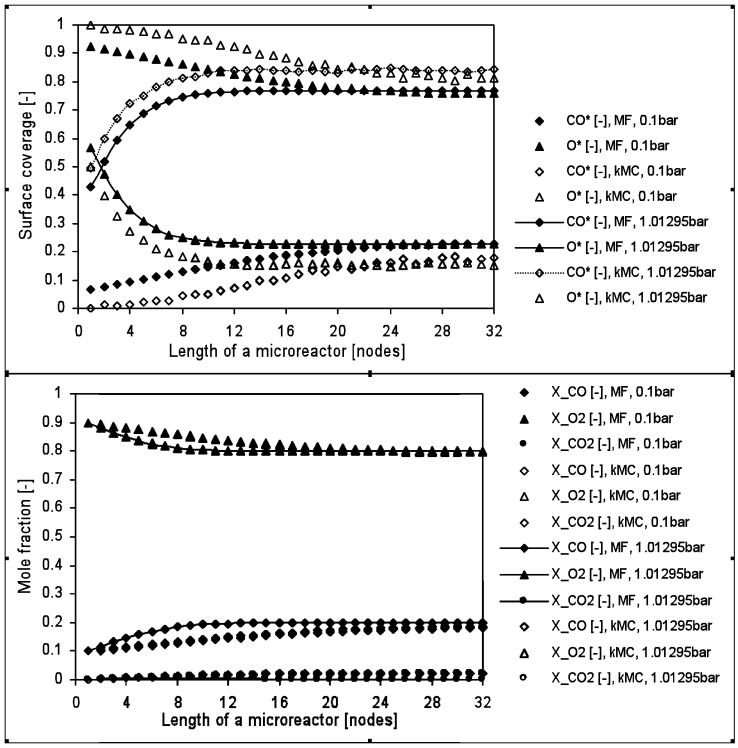

Figure 3: Comparison of (a) surface coverages and (b) gaseous mole fractions at the catalytic surface for the mean field (MF) and the multi-scale FD – kMC models at t=0.01s.

(a)

(b)

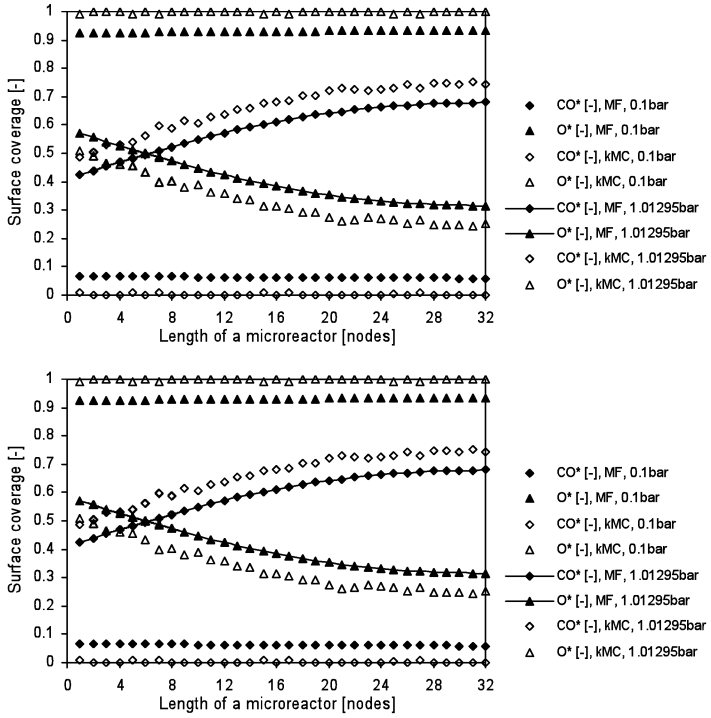

Figure 4: Comparison of (a) surface coverages and (b) gaseous mole fractions at the catalytic surface for the mean field (MF) and the multi-scale FD – kMC models at t=0.2 s.

Figure 5 and 6 depict the effect of inlet velocity on surface coverages and surface gaseous mole fractions at the catalytic surface at *0.01 s* and *0.2 s*, respectively (P=0.1 bar and T=700 K). If the inlet velocity increases from v=0.0 m/s, to 0.1 m/s, the difference from the MF model is almost negligible, while some difference can be observed for the FD-kMC model for t=0.01s as depicted in Figure 5a. There are no visible differences for t=0.2 s (Figure 6a). The corresponding gaseous mole fractions at the reactive surface are shown in Figure 5b and 6b. The change of inlet velocity has no effect on the mole fractions of CO, O_2 and CO_2, simulated with both models.

(a)

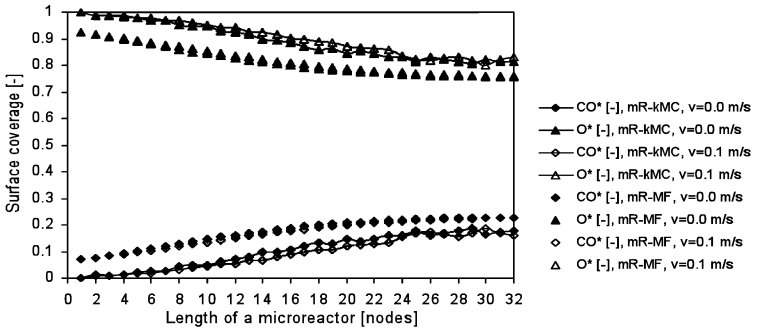

(b)

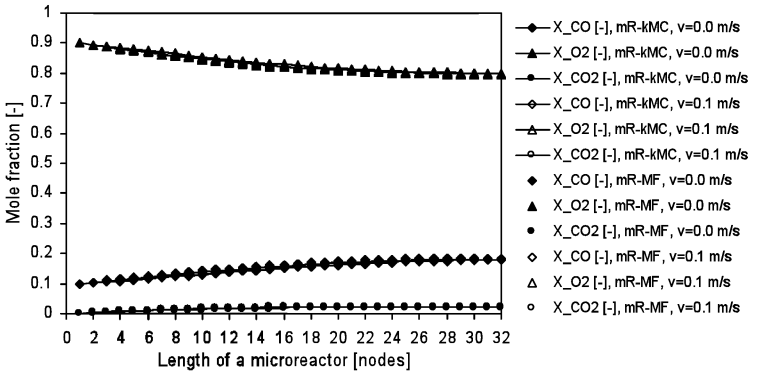

Figure 5: Comparison of (a) surface coverages and (b) gaseous mole fractions at the catalytic surface for the MF and the multi-scale FD – kMC models at different inlet velocities and t=0.01s.

The last parametric study for the *CO* oxidation mechanism is performed at *0.1 bar*, *700 K* and at mole fraction $X_{CO}=0.285$ and $X_{O2}=0.715$ with inlet boundary conditions $X_{CO}=0.1$ and $X_{O2}=0.9$. All other data are the same as for the previous case study. Figure 7 and 8 depict surface coverages and gaseous mole fractions at the catalytic surface at *0.01 s* and *0.2 s* for the MF and the FD–kMC model. By changing the initial mole fraction of *CO* from *0.2* to *0.285* and that of O_2 from *0.8* to *0.715* the models show different behaviour at P=*0.1 bar*, compared to Figure 3 and 4. The multi-scale model predicts lower *O** coverage from the MF model at the entrance of the microreactor, but higher *O** coverage from the middle and onwards. The reverse differences are observed for *CO** coverage. This case shows that the multi-scale model can predict not only quantitative, but also potentially qualitative differences from the corresponding MF model for the range of parametric conditions investigated.

4. CONCLUSIONS

A multi-scale model of a microreactor with a catalytic wall has been presented, which combines a macroscopic FD-based model of the bulk gaseous phase and a series of microscopic kMC lattices, which simulate the surface dynamics, including adsorption, desorption and surface reactions. The length-scales are coupled through the boundary conditions at the reactive surface equating the net number of gaseous particles adsorbing/desorbing to the diffusive flux into the reactive surface. The model is parallelised using MPI for efficient computation. A number of parametric studies have shown that the FD-kMC model shows the same trends as the MF model with quantitative differences on surface coverages for a number of parameters, but can also predict qualitative differences for different conditions. In a forthcoming publication we will explore the effects of surface diffusion and we will include effective communication between adjacent kMC lattices to account for the lateral diffusive movement of surface species.

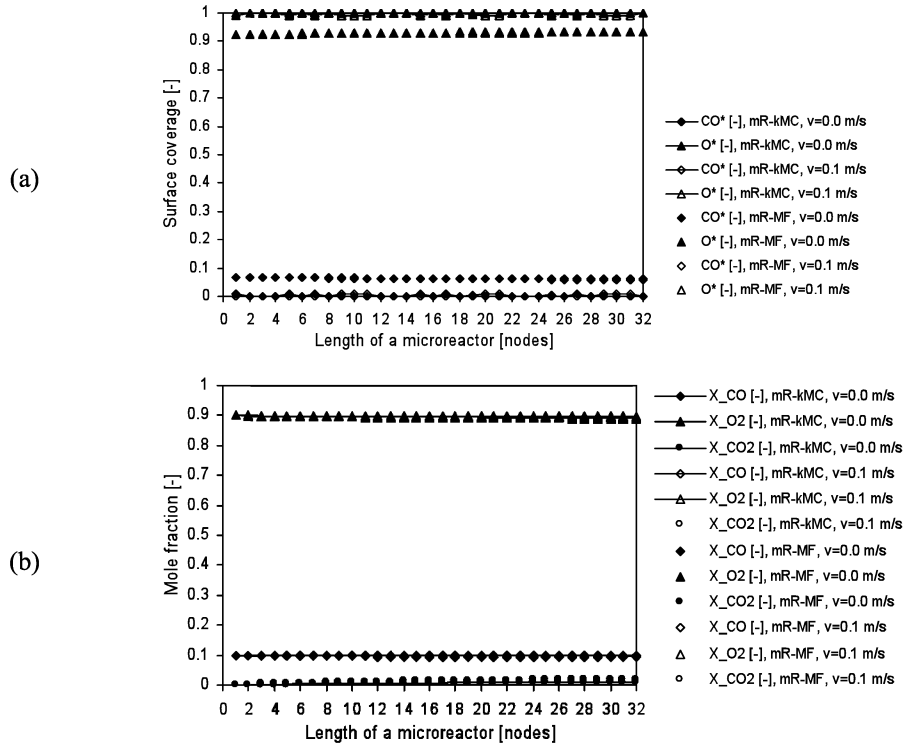

Figure 6: Comparison of (a) surface coverages and (b) gaseous mole fractions at the catalytic surface for the mean MF and the multi-scale microreactor FD – kMC models at different inlet velocities and t=0.2 s.

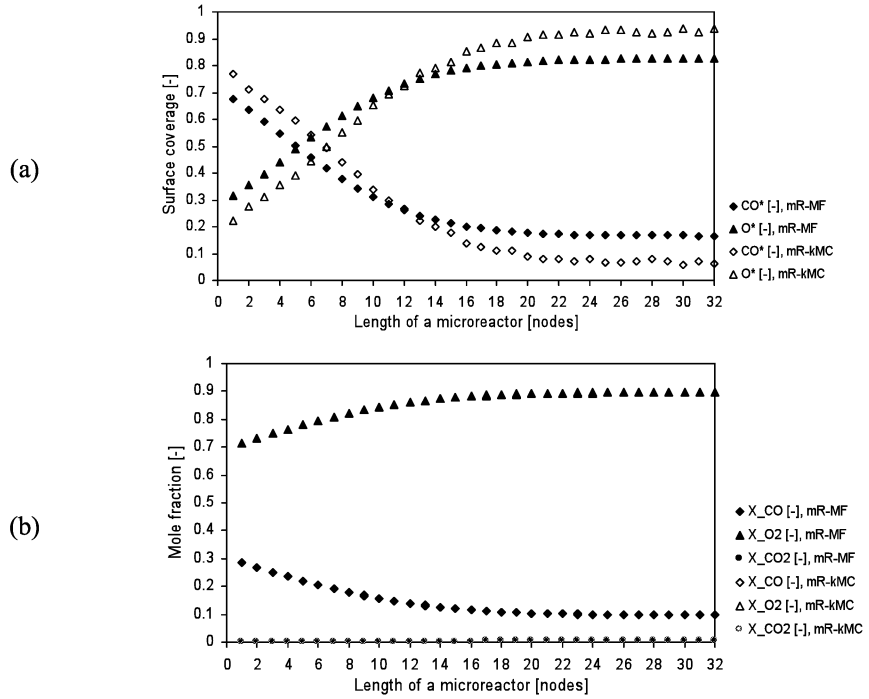

Figure 7: Comparison of (a) surface coverages and (b) gaseous mole fractions at the catalytic surface for the mean field (MF) and the multi-scale microreactor FD – kMC models at different inlet velocities and t=0.01s.

(a)

(b)

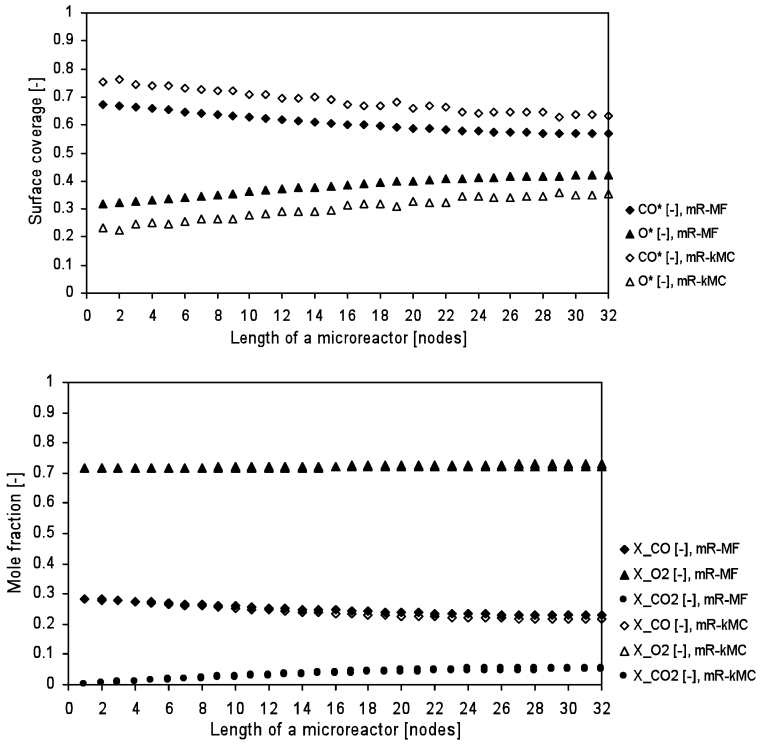

Figure 8: Comparison of (a) surface coverages and (b) gaseous mole fractions at the catalytic surface for the mean field (MF) and the multi-scale microreactor FD – kMC models at different inlet velocities and t=0.2 s.

5. REFERENCES

Ehrfeld W., Hessel V., Lowe H. (2000). Microreactors: New technology for modern chemistry, Wiley-VCH, Weinheim.

Majumder D and Broadbelt LJ (2006) AIChE J, 52, 4214.

Poling B.J., Prausnitz J.M., O'Connell J.P. (2001). The properties of gases and liquids, fifth edition, McGraw-Hill, New York.

Raimondeau S., Vlachos D.G. (2002). Comput. Chem. Eng. 26, 965.

Reese J.S., Raimondeau S., Vlachos D.G. (2001). J. Comput. Phys. 173, 302.